

## Modeling and simulation of a photovoltaic generator for analyzing the impact of faults on the I-V curve

 Guy M. Toche Tchio<sup>1\*</sup>, Joseph Kenfack<sup>3</sup>, Joseph Voufo<sup>3</sup>, Sanoussi S. Ouro-Djobo<sup>1,2</sup>

<sup>1</sup>Regional Center of Excellence for Electricity Management (CERME), University of Lomé, Togo; mtoche6@gmail.com (G.M.T.T.).

<sup>2</sup>Solar Energy Laboratory, Department of Physics, Faculty of Sciences, University of Lomé, Togo.

<sup>3</sup>Laboratory on Small hydropower and hybrid systems, National Advanced School of Engineering of Yaoundé (NASEY), University of Yaoundé 1, Cameroon; joskenfack@yahoo.fr (J.K.), voufojo1@gmail.com (J.V).

---

**Abstract:** The rapid expansion of the solar industry has underscored the importance of photovoltaic installations in the ongoing transition to sustainable energy. With this growth comes the crucial task of effectively monitoring and controlling the power generated. Photovoltaic systems are particularly vulnerable to defects due to their exposure to challenging environmental conditions, which can lead to reduced power output and an increased risk of fire. Therefore, a thorough analysis of any faults is essential in order to mitigate potential damage to the system. The present study proposes a comprehensive analysis of the behavior of a photovoltaic generator comprising four modules. MATLAB/Simulink software is used to model the generator in healthy operation. Subsequently, a simulation of the generator in faulty conditions is conducted, considering four fault cases: partial shading (PS), open circuit fault (OCF), bypass diode disconnected (PSBD), and twinned fault bypass diode disconnected plus open circuit (PSBDOC). A detailed examination of the simulation results for the faults above reveals that the twinned fault results in a substantial reduction in the output current, as well as an elimination of the open circuit voltage of the photovoltaic generator. This contrasts the behavior observed in a system comprising two modules, wherein the open circuit voltage remains unaltered. This particular fault offers a compelling rationale for the monitoring of photovoltaic installations, to enhance overall productivity while avoiding any potential damage to the system.

---

**Keywords:** *Faults, Modeling, Photovoltaic generator, Simulation.*

### 1. Introduction

#### 1.1. Motivation

In a context marked by the promotion of access to reliable, sustainable, modern, and affordable energy services [1], the pace of development of renewable energies is increasing. Among these energies, photovoltaic solar power has experienced significant growth in recent decades. This growth is supported by factors such as reduced production costs, government policies, and the need for alternatives to fossil fuels [2]. Alternatively, solar power can be adapted to various geographical areas, including remote and impassable regions. Its non-polluting nature, ease of implementation, low maintenance cost, and durability make it an attractive option. There's also a growing interest in using solar power to enhance the reliability of electrical systems through decentralized energy sources [3]. Despite their numerous advantages, photovoltaic systems often operate at less than full capacity due to exposure to harsh environmental and climatic conditions. This can lead to faults in PV modules, cables, and inverters, which, if not detected in time, can result in power loss, fire risk, or complete system shutdown [4]. It is crucial to analyze the behavior of the PV generator to identify and eliminate any

anomalies that may pose safety hazards and fire risks [5]. After the installation of a PV system, it is crucial to implement systematic monitoring to guarantee optimal operation. This process entails technicians performing field measurements to identify and rectify any potential faults. This proactive approach also inspires researchers to improve system reliability through the analysis of characteristic I-V curves [6]. The analysis of IV or PV characteristics is an essential process for understanding fault scenarios and their impact on parameters such as open circuit voltage ( $V_{oc}$ ) and the short-circuit current ( $I_{sc}$ ), the voltage and the current at the maximum power point ( $V_{mpp}, I_{mpp}$ ) [7]. The examination of PV generator behavior under faulty conditions begins with identifying and categorizing faults based on their frequency. According to Toche et al. [2], environmental and electrical faults are the most common and hazardous for PV systems. The authors explain that undetected environmental faults can lead to electrical faults.

### 1.2. Related Literature

Several methods have been proposed in the literature to detect and locate defects in photovoltaic (PV) systems. These methods include visual, thermal, and electrical approaches [2, 4]. Among these, electrical methods utilizing electrical signatures are considered more advantageous and promising for analyzing and diagnosing PV systems [6, 7]. Shah et al. [10] have proposed a modeling and simulation technique based on MATLAB/Simulink to implement and determine the characteristics of a PV module and its performance under different irradiation and temperature values. A hybrid approach based on classification algorithms has been used to predict the output power of a PV system by combining the one-diode model and the two-diode model of a solar cell [11]. An experimental study on a 1.5 kW PV field was conducted to detect diode bypass, module faults, and mismatch faults using electrical parameters [12]. Additionally, modeling a PV system using MATLAB/Simulink has provided data on physical and electrical faults [9]. This data was utilized to train the Random Forest algorithm to detect and classify the defects. The results indicate that the proposed model has an accuracy of 98.6% for defect detection and 94.2% for classification. Hammond et al. [13] proposed three independent applications to evaluate the impact of dirt on PV modules. Modeling the electrical performance of a generator under constant electrical loads made it possible to determine the current/voltage operating point of the PV module for each electrical load [14]. A simulation procedure of a PV cell/module/field is proposed using MATLAB/Simulink tools to analyze the characteristics of a PV system under different operating conditions [15]. Novel analytical methods have been developed for identifying shading defects, non-shading zero-yield faults, and brief zero-yield faults [16]. The use of MATLAB/Simulink has allowed for analyzing the functionality of solar cells under different temperature and irradiance conditions, enabling a comprehensive assessment of solar module performance across various environmental scenarios [17]. To predict solar energy production, a photovoltaic (PV) module based on the Bishop model was simulated using MATLAB/Simulink software under a range of irradiation and temperature conditions [18, 19]. Compaoré et al [20], studied the impact of faults in a photovoltaic generator. Furthermore, a methodology based on the complete IV characteristic has been proposed for evaluating the performance of the PV module under fault conditions [21]. The analysis of the presented work shows that the authors' primary goal was to model the generator to forecast the output power of PV modules. However, research on simulating modules under faulty conditions has mainly focused on relatively simple defects such as shading and degradation of the PV module. The study of the impact of accumulated defects has not been sufficiently addressed. Nonetheless, some authors have examined the condition of a system consisting of two PV modules, emphasizing the impact of an accumulated bypass diode fault with an open circuit [22]. The authors illustrate that this fault is similar to the open circuit fault in this configuration of two modules in parallel, although confirmation on a larger system is needed. The aim of this paper is to analyze the impact of partial shading (PS), open circuit (OCF), bypass diode disconnected (PSBD), and paired bypass diode disconnected plus open circuit (PSBDOC) faults on the parameters of generator output for multiple PV modules.

### 1.3. Contribution

The main contribution of this paper is to examine the influence of a twin fault on a series-parallel circuit of a photovoltaic generator:

- Examine the effects of the twin fault (PSBDOC) on a four PV modules system
- Contrast the impact of this issue with that identified in a two PV modules system

Section 2 of the paper outlines the modeling of a PV generator under normal conditions, section 3 focuses on simulating the various selected faults, and section 4 is dedicated to presenting the results and discussions.

## 2. Modeling a PV Generator

When modeling a PV generator, it's essential to factor in scale parameters such as the number of cells per module, the number of modules connected in series per string, and the number of strings in parallel. Additionally, understanding electrical parameters is crucial for accurate modeling,  $V_{oc}$ ,  $I_{sc}$ ,  $V_{mpp}$ ,  $I_{mpp}$ , the temperature coefficient in open circuit ( $k_v$ ) and short circuit ( $k_i$ ). In our analysis, we will assess the health of the PV generator based on its configuration and the specific symptoms associated with each fault in the characteristic IV curve. We will focus on a PV system consisting of four PV modules and model four different fault scenarios to generate the IV curve. This particular configuration is chosen to highlight the similarities between the symptoms of open circuit faults (OCF) and the twin fault (PSBDOC) observed in two PV modules connected in parallel [22]. The construction of this generator is based on repetition and combination of blocks from the solar cell

### 2.1. Modeling a Solar Cell

In the existing literature on solar cell equivalent circuits, the single-diode model is widely used and has been shown to produce satisfactory results [23]. The electrical circuit of this model is composed of a current source  $I_{ph}$  delivered by the sunlight received on the surface of the cell and a current diode  $I_d$  which provides an unilluminated PN junction. The series resistance ( $R_s$ ) represents the contact and connection resistance, taking into account the ohmic losses of materials and semiconductors. This ensures the interconnection between cells. A shunt resistor ( $R_s$ ) is included to represent the leakage current of the PN junction, which is placed in parallel with the diode. Additionally, a voltage source (V) is incorporated to provide the output voltage of the cell. In a study by Ding et al [24], a single-diode model was proposed for use in modelling photovoltaic modules using MATLAB/Simulink. Figure 1 shows the equivalent circuit of a single diode solar cell consisting of five parameters ( $I_{ph}$ ,  $I_0$ ,  $R_s$ ,  $R_{sh}$ ,  $n$ ).

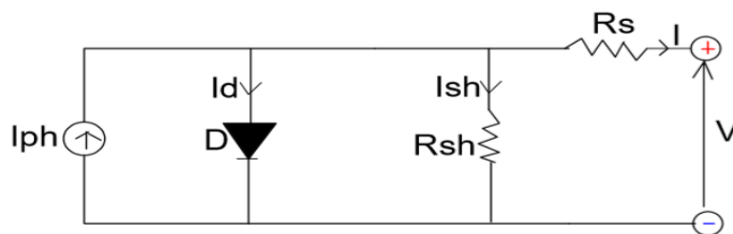


**Figure 1.**  
Electrical circuit of a single diode solar cell.

The general equation of a cell to a diode is given by equation (1) applying Kirchhoff's law

$$I = I_{ph} - I_d - I_{sh} \quad (1)$$

$$I_{ph} = [I_{scn} + k_i(T_c - T_n)] \frac{G}{Gn} \quad (2)$$

$$I_d = I_0 \left\{ \exp\left(\frac{V}{nV_T}\right) - 1 \right\} \quad (3)$$

In a short circuit situation, the photo current  $I_{ph}$  is confused with the short circuit current  $I_{sc}$  as shown in equation (3) for  $V = 0$

$$I = I_{sc} - I_0 \left\{ \exp\left(\frac{V}{nV_T}\right) - 1 \right\} \quad (4)$$

- $I_0$  : The saturation current of the diode is the asymptotic value of the current in reverse bias. It depends only on the temperature and is given by the relation (4)

$$I_0 = I_{01} \left[ \frac{T_c}{T_n} \right]^3 e^{\frac{qEg}{nK} \left( \frac{1}{T_n} - \frac{1}{T} \right)} \quad (5)$$

- $I_{01}$  : reverse saturation current of the diode given by (5)

$$I_{01} = \frac{I_{sc}}{\left[ e^{\frac{qV_{oc}}{nKT}} - 1 \right]} \quad (6)$$

- $T_c = T_a + \frac{NOCT-20}{0.8} \times G$ : cell temperature
- $T_a$ : Ambient temperature
- $T_n$  : Outlet temperature in STC
- $K$  : Boltzmann constant  $1.3806503 \times 10^{-23}$  J/K
- $Eg$  : energy band 1.1ev
- $n$  : diode ideality factor between 1 and 2
- $ki = \frac{dI_{scn}}{dT}$ : temperature coefficient of short-circuit current
- $I_{01}$  : inverse saturation current of the diode given by the relation
- $V_T = \frac{kT_c}{q}$ : PN junction thermal voltage

The input current of the shunt resistor  $I_{sh}$  is given by the relationship below:

$$I_{sh} = \frac{V + IR_s}{R_{sh}} \quad (7)$$

By replacing the expressions in equation (8), the general equation of a photovoltaic cell is given by the following relationship:

$$I = I_{ph} - I_0 \left\{ e^{\left(\frac{V+IR_s}{nV_T}\right)} - 1 \right\} - \frac{V+IR_s}{R_{sh}} \quad (8)$$

- Expression of series resistance,  $R_s$

The increase in series resistance causes the current to drop rapidly. The impact of the voltage drop is not significant for the typical value of  $R_s$  since  $V + IR_s$  is always low,  $R_s$  determines the slope close to  $V_{oc}$  which can be used to determine  $R_s$ .

The power is maximum when  $\frac{dP}{dV} = 0$  and the solution to this equation at the point of maximum power has coordinates  $(V_{mp}, I_{mp})$  Thus,

$$\frac{dP}{dV} \Big|_{mp} = 0 \Leftrightarrow I_{mp} + V_{mp} \frac{dI}{dV} \Big|_{mp} = 0 \quad (9)$$

$$\frac{dI}{dV} \Big|_{mp} = -\frac{I_{mp}}{V_{mp}} \quad (10)$$

Furthermore, the derivative of (11) with respect to V is given by:

$$R_s = -\frac{dV}{dI} \Big|_{mp} (I_{mp} = 0, V_{mp} = V_{oc}) - \frac{1}{X_V} \quad (11)$$

$$X_V = \frac{I_0}{nV_T} \exp\left(\frac{V_{oc}}{nV_T}\right) \quad (12)$$

However, to power a large load in practice, the power delivered by the solar cell is insufficient, it is necessary to combine several cells in series or parallel in order to form a photovoltaic module capable of powering a load.

## 2.2. Modeling a PV Array

In free fault, the optimal voltage for a photovoltaic (PV) module is achieved by connecting multiple solar cells in series, assuming that the cells are all identical. Nevertheless, in the context of a photovoltaic field, an association of  $N_s$  modules in series and  $N_p$  string in parallel is carried out to obtain the current and the output voltage of the desired field as shown in Figure 2.

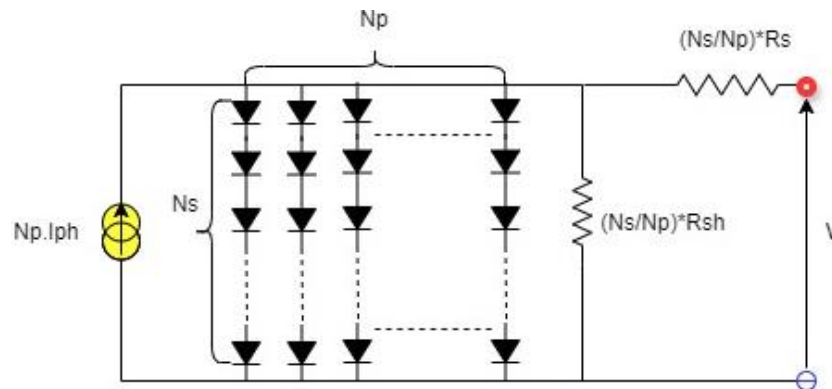


**Figure 2.**  
Modeling a PV generator.

Equations (13) and (14) show the relationships between the array output current as a function of voltage and the two parameters  $N_p$  and  $N_s$

$$I = N_p (I_{ph} - I_d) - I_{sh} \quad (13)$$

By substituting the diode current by its expression, we have the relation of the output current of the PV array.

$$I = N_p I_{ph} - N_p I_0 \left\{ e^{\left( \frac{\left( \frac{V}{N_s} + \frac{I}{N_p} R_s \right)}{nV_T} \right)} - 1 \right\} - \frac{V N_p / N_s + I R_s}{R_{sh}} \quad (14)$$

$$\begin{cases} I = N_p \times I_{string} \\ V = N_s \times V_{mod} \\ P = V \times I \end{cases} \quad (15)$$

$I$ : PV array output current

$V$ : PV array output voltage

### 3. Simulation of the PV System in Fault Conditions

The simulation of the various selected faults is performed according to the configuration shown in Figure 3.

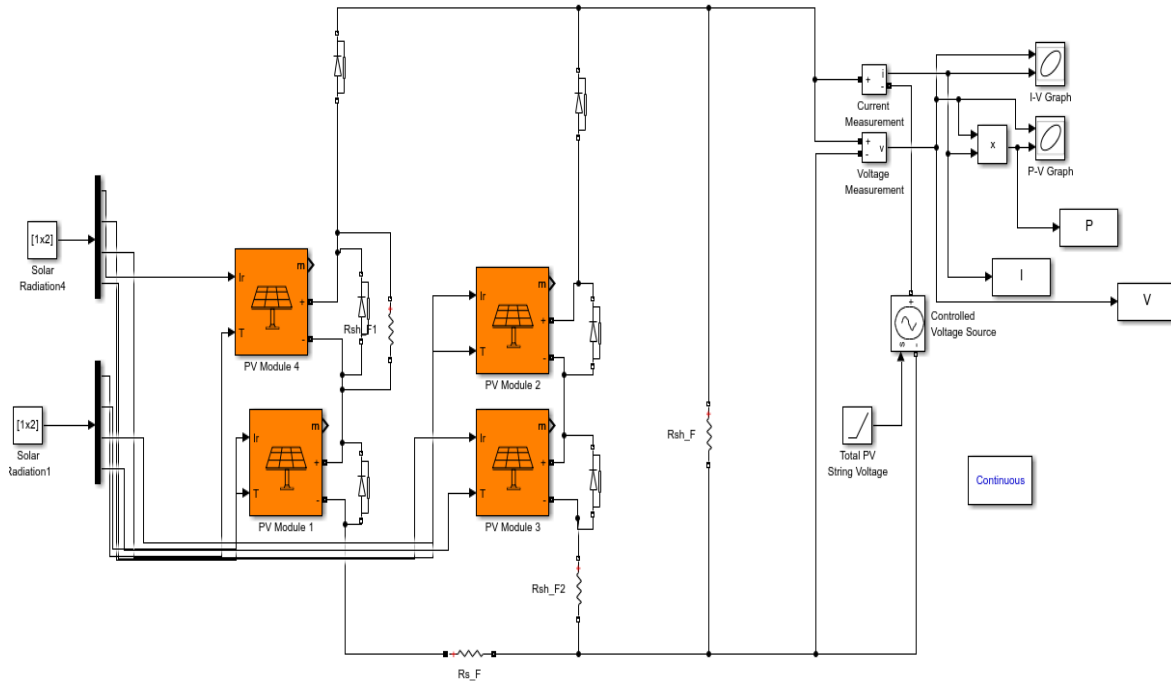


**Figure 3.**  
Structure of the PV array.

#### 3.1. Description of the PV generator

The photovoltaic (PV) generator under consideration in this study is composed of four solar modules, arranged in two chains of two modules in series. Each module is composed of 36 cells, which are divided into two groups of 18 cells. Each cell is protected by a bypass diode. The photovoltaic (PV) module employed in this study is a product of the BLD SOLAR brand. The technical specifications of this module are presented in Table 1.

**Table 1.**  
Technical specification of the BLD SOLAR monocrystalline solar module

Electrical parameters	Values
Nominal power ( $P_{mp}$ )	50W
Open circuit voltage ( $V_{OC}$ )	22.1V
Short circuit current ( $I_{SC}$ )	2.81A

Voltage at maximum power ( $V_{mp}$ )	18.1V
Current at maximum power ( $I_{mp}$ )	2.76 A
Number of cells	36

### 3.2. Fault configuration

The configuration of different faults is accomplished through the utilization of the gain block in conjunction with supplementary resistors. Four distinct types of defects are considered in this analysis, which excludes the healthy case:

- Partial shading fault (PS): a module is obscured by adjusting the value of the block gain in an interval of  $[0 \ 100]$  to control the irradiation of the module. The occultation rate varies from 0 to 100%.
- Open circuit fault: a string is in open circuit if it is connected in series with a resistor
- Shading fault with bypass diode disconnected: module is obscured by adjusting the block gain and disconnecting the bypass diode
- Bypass diode disconnected plus open circuit, the module is blanked in an interval of  $[0 \ 1]$  corresponding to a rate of 0 to 100%, with the series connection of the  $R_{oc}$  resistor on the shaded string. Table 2. represents the summary of the different selected defects.

**Table 2.**

Setting parameters for different faults.

Faulty condition	PS degree (%)	$R_{SC}(\Omega)$	$R_{OC}(\Omega)$	$R_s(\Omega)$	$R_{sh}(\Omega)$
NF	0	$10^5$	$10^{-5}$	$10^{-5}$	$10^5$
PS 1 module	$[0-100]$	$10^5$	$10^{-5}$	$10^{-5}$	$10^5$
OCF 1 string	0	$10^5$	$10^5$	$10^{-5}$	$10^5$
PSBD 1 module	$[0-100]$	$10^5$	$10^{-5}$	$10^{-5}$	$10^5$
PSBDOC 1 module and 1 string	$[0-100]$	$10^5$	$10^5$	$10^{-5}$	$10^5$

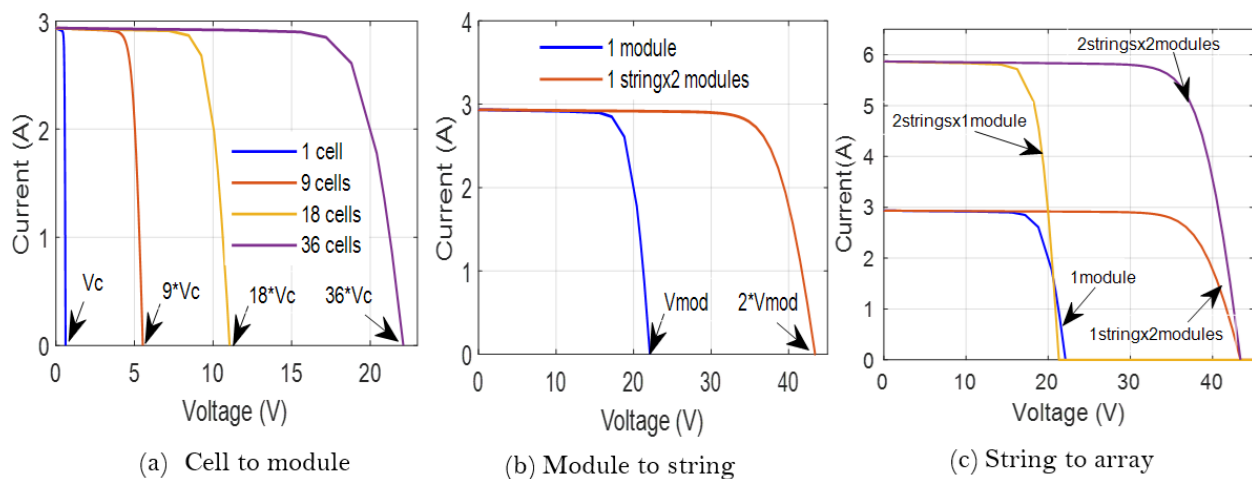


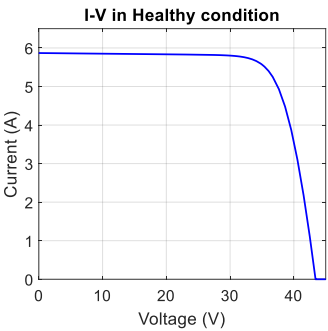
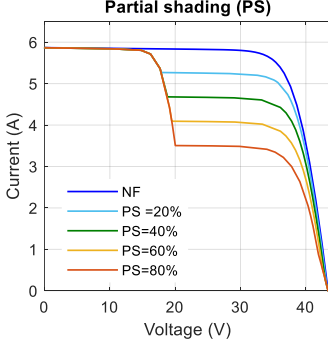
**Figure 4.** Behavior of a PV generator under different configurations.

### 4. Results and Discussion

#### 4.1. Symptom Analysis in Free Fault

Figure 2 illustrates that the placement of the GPV in series increases the open circuit voltage ( $V_{oc}$ ), while its placement in parallel increases the value of the short circuit current ( $I_{sc}$ ), regardless of the configuration of the PV generator. To illustrate, in the transition from the cell to the module (Figure 4a), the module voltage is 36 times that of the cell, or 22.1 V, corresponding to approximately  $0.61 \times 36$ . A similar phenomenon occurs at the level of. Figure 4b illustrates a scenario where the voltage of the string is equal to twice that of the module, or 44.2 V, corresponding to approximately  $22.1 \times 2$ . However, when we transition from the string to the PV field (Figure 4c), the voltage and current increase due to the series-parallel configuration of the modules. This increase is proportional to the number of modules in a string and the number of parallel strings in the PV field. Figure 4c illustrates a short-circuit current of 5.86A, which corresponds to  $2 \times 2.93A$ .

**Table 2.**  
Impact of defects on characteristic IV.

Condition	Impact on curve IV	Symptoms
NF	None	 <p>The graph titled "I-V in Healthy condition" plots Current (A) on the y-axis (0 to 6) against Voltage (V) on the x-axis (0 to 40). The curve shows a constant current of approximately 6A up to about 35V, followed by a sharp drop to 0A at approximately 42V.</p>
P.S.	<p>Appearance of an inflection point about 1/2 of <math>V_{oc}</math> the healthy condition as there are two modules in a string with one module shaded. The current at the inflection point is weaker as the degree of shading is greater.</p> $V_{oc(PS)} = \frac{1}{2} V_{oc(NF)}$	 <p>The graph titled "Partial shading (PS)" plots Current (A) on the y-axis (0 to 6) against Voltage (V) on the x-axis (0 to 40). It shows five curves: NF (blue), PS=20% (cyan), PS=40% (green), PS=60% (yellow), and PS=80% (orange). Each curve shows a step-like decrease in current at different voltage points, with the inflection point occurring at approximately half the open-circuit voltage of the healthy condition. The legend indicates: NF (blue), PS=20% (cyan), PS=40% (green), PS=60% (yellow), PS=80% (orange).</p>

<p>OCF</p>	<p>The current <math>I_{sc}</math> in the presence of the open circuit fault decreases by <math>\frac{1}{2}</math> of that <math>I_{sc}</math> in healthy condition</p> $I_{sc(OCF)} = \frac{1}{2} I_{sc(NF)}$ <p>During this time, the open circuit voltage remains unchanged.</p>	
<p>PSBD</p>	<p>The current <math>I_{sc}</math> in the presence of the partial shading fault with bypass diode disconnected decreases by <math>\frac{2}{3}</math> of that <math>I_{sc}</math> in healthy condition</p> $I_{sc(PSBD)} = \frac{2}{3} I_{sc(NF)}$ <p>The open circuit voltage remains unchanged during this period</p>	
<p>PSBDOC</p>	<p>The current <math>I_{sc}</math> in the presence of the partial shading fault with bypass diode disconnected and open circuit decreases by <math>\frac{1}{2}</math> of that <math>I_{sc}</math> in healthy condition</p> $I_{sc(PSBDOC)} = \frac{1}{2} I_{sc(NF)}$ <p>The open circuit voltage in this case is zero (<math>V_{oc(PSBDOC)} = 0 V</math>)</p>	

4.2. Symptom Analysis in Faulty Condition

However, in the case where the PV generator is composed of two modules mounted in parallel, this voltage is no longer zero, the fault becomes similar to the open circuit fault [22]. The figure 5 illustrates the similarity between the two fault cases with two modules connected in parallel

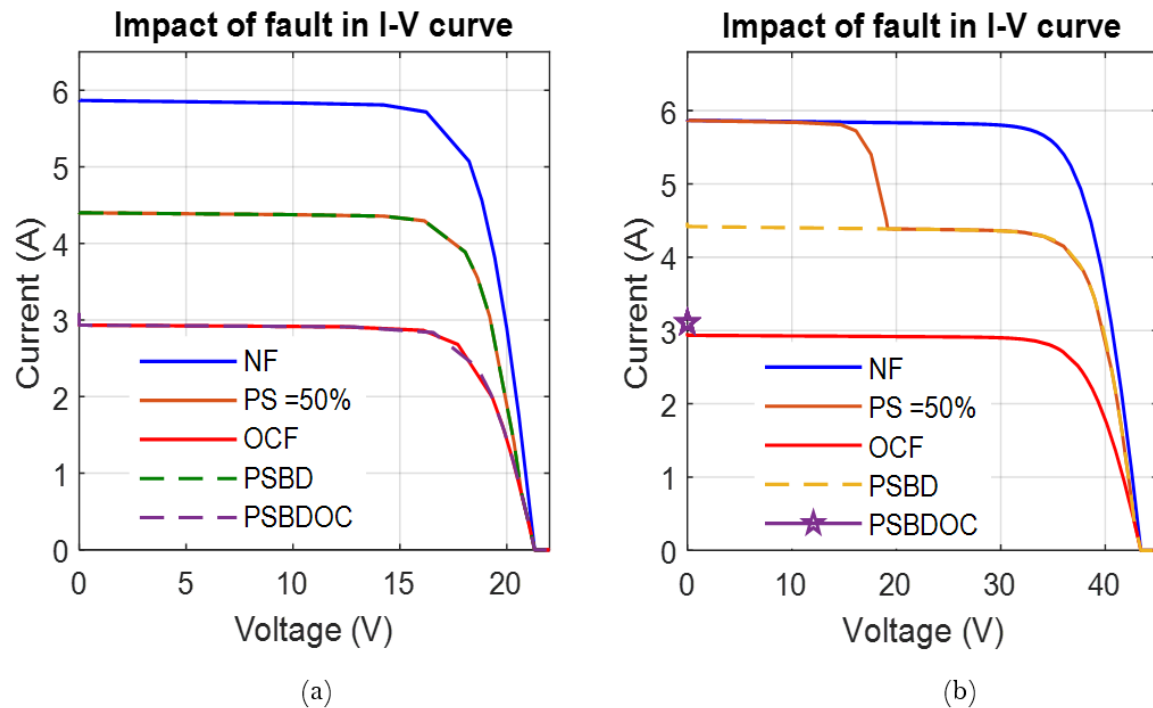


**Figure 5.**  
(a) Two modules in parallel, (b) Four modules 2stringsx2modules.

As mentioned in the work of Toche et al. [22], in a system comprising two modules operating in parallel, the open circuit fault and the twin fault manifest similar symptoms on curve IV. Indeed, a reduction in the short-circuit current is observed, despite a constant open circuit voltage. Moreover, in this identical configuration, the partial shading fault (PS) and the partial shading fault with bypass diode disconnected (PSBD) also manifest with identical symptoms. A distinction between these faults becomes apparent when the number of modules in the string is increased. To illustrate, in our configuration (Figure 5b), the OCF and PSBDOC faults exhibit identical short-circuit current values but distinct open-circuit voltages. In contrast to the open circuit voltage of the OCF fault, which remains constant, the open circuit voltage of the PSBDOC fault is zero. A similar observation is made at the level of the partial shading fault and the disconnected bypass diode, where an inflection point is noted in relation to the reduction in the short-circuit current and the open circuit voltage. In contrast, the open circuit voltage remains constant in an open circuit fault situation (Figure 5a).

## 5. Conclusion

The present paper describes the simulation of a photovoltaic (PV) system comprising four PV modules in the MATLAB/Simulink environment. Four additional fault cases were simulated outside the normal case, namely partial shading faults, open circuit, disconnected bypass diode and twin faults. A comprehensive examination was conducted to ascertain the influence of the various defects on the IV curve. A comparative analysis of the proposed configuration with the configuration of two modules mounted in parallel revealed that the twin fault and the open circuit fault are similar only in the configuration of two PV modules. Furthermore, in the proposed configuration, an open circuit fault results in a reduction in the short circuit current with a constant open circuit voltage. In contrast, this open circuit voltage is cancelled in the presence of a twin fault (PSBDOC). Nevertheless, future work should integrate an MPPT converter to enhance this simulation strategy. This will facilitate the real-

time evaluation of the impact of a series of paired faults on a large field comprising more than four PV modules. The aforementioned conclusions were drawn.

### Funding:

This work was supported by the World Bank, through the Regional Center of Excellence for Electricity Management (CERME).

### Acknowledgements:

The authors are deeply grateful to the World Bank for funding this research through CERME (Regional Center of Excellence for Electricity Management). We also thank the reviewers for their insightful and positive comments and suggestions, which have greatly helped us improve this article.

### Author contributions:

GMTT worked on the research paper, JK, JV participated in proofreading the paper and SSO-D carried out supervision. All authors have read and accepted the published version of the manuscript.

### Copyright:

© 2024 by the authors. This article is an open access article distributed under the terms and conditions of the Creative Commons Attribution (CC BY) license (<https://creativecommons.org/licenses/by/4.0/>).

### References

- [1] “Integration of the 2030 Agenda for Sustainable Development Guidance note to ( PDFDrive ) (1)”.
- [2] G. M. Toche Tchio, J. Kenfack, D. Kassegne, F.-D. Menga, and SS Ouro-Djobo Appl Sci, “A Comprehensive Review of Supervised Learning Algorithms for the Diagnosis of Photovoltaic Systems, proposing a New Approach Using an Ensemble Learning Algorithm”, *Applied Sciences*, vol. 14, n°5, p.2072, doi: 10.3390/ app14052072.
- [3] M. Sabbaghpur Arani and M. A. Hejazi, “The comprehensive study of electrical faults in PV arrays,” *Journal of Electrical and Computer Engineering*, vol. 2016, 2016, doi: 10.1155/2016/8712960.
- [4] T. K. Takashima, J. Yamaguchi, K. Otani, K. Kato, and M. Ishida, “experimental studies of failure detection methods in pv module strings.”
- [5] S. R. Madeti and S. N. Singh, “A comprehensive study on different types of faults and detection techniques for solar photovoltaic system,” 2017, *Elsevier Ltd.* doi: 10.1016/j.solener.2017.08.069.
- [6] H. Al Mahdi, P. G. Leahy, and A. P. Morrison, “Experimentally derived models to detect onset of shunt resistance degradation in photovoltaic modules,” *Energy Reports*, vol. 10, pp. 604–612, Nov. 2023, doi: 10.1016/j.egy.2023.07.019.
- [7] X. Chen, M. Jiang, K. Ding, Z. Yang, J. Zhang, L.Cui and H. M. Hasanien., “Fault Pre-diagnosis, Type Identification and Degree Diagnosis Method of the Photovoltaic Array Based on the Current-Voltage Conversion,” *IEEE Trans Power Electron*, 2024, doi: 10.1109/TPEL.2024.3427649.
- [8] W.-T. Lin, C.-M. Chang, Y.-C. Huang, C.-C. Wu, and C.-C. Kuo, “Fault Diagnosis in Solar Array IV Curves Using Characteristic Simulation and Multi-Input Models,” *Applied Sciences*, vol. 14, no. 13, p. 5417, Jun. 2024, doi: 10.3390/app14135417.
- [9] S. S. SYED, B. Li, and A. Zheng, “Detection and Classification of Physical and Electrical Fault in PV Array System by Random Forest-Based Approach,” *International Journal of Electrical, Energy and Power System Engineering*, vol. 7, no. 2, pp. 67–84, Jun. 2024, doi: 10.31258/ijeepse.7.2.67-84.
- [10] M.W. Shah and R.L. Biata, “Design and Simulation of Solar PV Model Using Matlab /Simulink,” *International Journal of Scientific & Engineering Research*, vol. 7, no. 3, p. 551-554, 2016. [Online]. Available: <http://www.ijser.org>
- [11] M. Malvoni and Y. Chaibi, “Machine learning based approaches for modeling the output power of photovoltaic array in real outdoor conditions,” *Electronics (Switzerland)*, vol. 9, no. 2, Feb. 2020, doi :10.3390/electronics9020315.
- [12] M. Dhakshinamoorthy, K. Sundaram, P. Murugesan, and P. W. David, “Bypass diode and photovoltaic module failure analysis of 1.5kW solar PV array,” *Energy Sources, Part A: Recovery, Utilization and Environmental Effects*, vol. 44, no. 2, pp. 4000–4015, 2022, doi: 10.1080/15567036.2022.2072023.
- [13] R. Hammond, D. Srinivasan, A. Harris, and K. Whitfield, “Effects of soiling on PV module and radiometer performance”, *IEEE*, p. 1121-1124, 1997
- [14] E. M. Salilih and Y. T. Birhane, “Modeling and Analysis of Photo-Voltaic Solar Panel under Constant Electric Load,” *Journal of Renewable Energy*, vol. 2019, p. 1–10, Aug. 2019, doi: 10.1155/2019/9639480.

- [15] X. H. Nguyen and M. P. Nguyen, "Mathematical modeling of photovoltaic cell/module/arrays with tags in Matlab /Simulink," *Environmental Systems Research*, vol. 4, no. 1, Dec. 2015, doi: 10.1186/s40068-015-0047-9.
- [16] S. K. Firth, K. J. Lomas, and S. J. Rees, "A simple model of PV system performance and its use in fault detection," *Solar Energy*, vol. 84, no. 4, pp. 624–635, Apr. 2010, doi: 10.1016/j.solener.2009.08.004.
- [17] B. Cirak, "Modelling and Simulation of Photovoltaic Systems Using MATLAB / Simulink," *WSEAS Transactions on Power Systems*, vol. 18, p. 49–56, 2023, doi: 10.37394/232016.2023.18.6.
- [18] V. Vai, S. Chhorn, R. Chhim, S. Tep, and L. Bun, "Modeling and Simulation of PV Module for Estimating Energy Production under Uncertainties," in *2020 8th International Electrical Engineering Congress, iEECON 2020*, Institute of Electrical and Electronics Engineers Inc., Mar. 2020. doi: 10.1109/iEECON48109.2020.229578.
- [19] G. S. Reddy, T. B. Reddy, and M. V. Kumar, "A MATLAB based PV Module Models analysis under Conditions of Nonuniform Irradiance," in *Energy Procedia*, Elsevier Ltd, 2017, pp. 974–983. doi: 10.1016/j.egypro.2017.05.218.
- [20] O. W. Compaore, G. Hoblos, and Z. Koalaga, "Analysis of the impact of faults in a photovoltaic generator."
- [21] B. Li, C. Delpha, A. Migan-Dubois, and D. Diallo, "Fault diagnosis of photovoltaic panels using full I–V characteristics and machine learning techniques," *Energy Convers Manag*, vol. 248, Nov. 2021, doi: 10.1016/j.enconman.2021.114785.
- [22] G. M. Toche Tchio, J. Kenfack, J. Voufo, Y. A. Mindzié, and S. S. Ouro-Djobo, "Diagnosing faults in a photovoltaic system using the Extra Trees ensemble algorithm," *Aims Energy*, 12(4),727-750, doi: 10.3934/energy.2024034
- [23] S. Obukhov, I. Plotnikov, and M. Kryuchkova, "Simulation of Electrical Characteristics of a Solar Panel," in *IOP Conference Series: Materials Science and Engineering*, Institute of Physics Publishing, Jun. 2016. doi :10.1088/1757-899X/132/1/012017.
- [24] J. Zhang, Z. Yang, K. Ding, L. Feng, F. Hamelmann, X. Chen, Y. Liu and L. Chen, "Modeling of Photovoltaic Array Based on Multi-Agent Deep Reinforcement Learning Using Residuals of I–V Characteristics," *Energies (Basel)*, vol. 15, no. 18, Sep. 2022, doi :10.3390/en15186567.